

Anti-trypanosomal activity of doubly modified salinomycin derivatives

Michał Antoszczak ^{a,*}, Dietmar Steverding ^b, Michał Sulik ^a, Jan Janczak ^c, Adam Huczyński ^a

^a Department of Bioorganic Chemistry, Faculty of Chemistry, Adam Mickiewicz University, Umultowska 89b, 61–614 Poznań, Poland

^b Bob Champion Research & Education Building, Norwich Medical School, University of East Anglia, Norwich, UK

^c Institute of Low Temperature and Structure Research, Polish Academy of Sciences, PO Box 1410, 50–950 Wrocław, Poland

Keywords: Polyether ionophores; Allylic hydroxyl oxidation; Reductive amination; Anti-parasitic activity; African trypanosomiasis; *Trypanosoma brucei*; Crystal structure

Corresponding Author

* E-mail: michant@amu.edu.pl (M. Antoszczak)

Abstract: As a group of biologically active compounds, polyether antibiotics (ionophores) show a broad spectrum of interesting pharmacological properties, ranging from anti-bacterial to anti-cancer activities. There is increasing evidence that ionophores, including salinomycin (**SAL**), and their semi-synthetic analogues are promising candidates for the development of drugs against parasitic diseases. Our previous studies have shown that esterification and amidation of the C1 carboxylate moiety of **SAL** provides compounds with potent activity against *Trypanosoma brucei*, protozoan parasites responsible for African trypanosomiasis. In this paper, we present the synthetic pathways, crystal structures and anti-trypanosomal activity of C1 esters, amides and hydroxamic acid conjugates of **SAL**, its C20-oxo and propargylamine analogues as well novel C1/C20 doubly modified derivatives. Evaluation of the trypanocidal and cytotoxic activity using bloodstream forms of *Trypanosoma brucei* and human myeloid HL-60 cells revealed that the single-modified C20-oxo and propargylamine precursor molecules **10** and **16** were the most anti-trypanosomal and selective compounds with 50% growth inhibition (GI₅₀) values of 0.037 and 0.0035 μM, and selectivity indices of 252 and 300, respectively. Also the salicylhydroxamic acid conjugate of **SAL** (compound **9**) as well as benzhydroxamic acid and salicylhydroxamic acid conjugates of **10** (compounds **11** and **12**) showed promising trypanocidal activities with GI₅₀ values between 0.032 to 0.035 μM but less favorable selectivities. The findings confirm that modification of **SAL** can result in derivatives with improved trypanocidal activity that might be interesting lead compounds for further anti-trypanosomal drug development.

1. Introduction

Polyether ionophores have been used in veterinary medicine for decades as non-hormonal growth promoters and as agents to control coccidiosis [1–2]. In addition to the industrial use of ionophores in animal husbandry [3], some of them show anti-fungal, anti-viral, and anti-cancer activity [4–6]. Salinomycin (**SAL**, **1**, **Scheme 1**), a polyether K⁺-selective membrane ionophore from *Streptomyces albus*, seems to be the most promising agent in this context as several studies have shown activity against different human cancer cells, multi-drug resistant cancer cells, cancer stem cells and human tumour xenograft models in mice [5]. Although accidental poisonings have been reported, **SAL** was found to improve the condition in a small group of cancer patients without any long-term acute adverse effects when used in the appropriate dose [5,7-8]. Mechanistically, the effects on several signal transduction pathways were suggested to explain the change in phenotype composition after **SAL** treatment, including Wnt signaling pathway involved in tumorigenesis and embryogenesis. Other pathways that were inhibited by **SAL** include KRas and modulation of Hedgehog signaling [5].

It should be pointed out that compounds that display anti-cancer activity, very often are also active against African trypanosomes [9]. These protozoan parasites cause sleeping sickness in humans and nagana disease in cattle [10–12], and are transmitted by the bites of infected tsetse flies (*Glossina* sp.) that are only found in rural regions of sub-Saharan Africa [13–14]. Historically, African trypanosomiasis has been a serious economic and public health problem in Africa, causing several epidemics over the last century [15]. According to the World Health Organization, the estimated number of actual cases is below 20,000, but the estimated population at risk is still 65 million people [16]. Because of nagana disease, livestock farming is difficult in many regions of sub-Saharan Africa and this is exacerbated by the rise of drug resistant

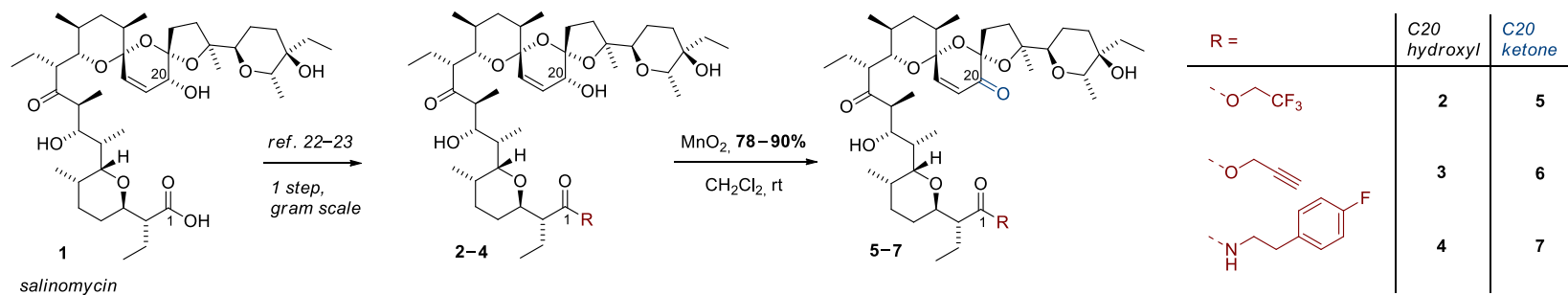
trypanosomes [10]. As the few drugs that are used for treatment of both sleeping sickness and nagana disease are outdated, have limited efficacy and may produce adverse side reactions [17–19], novel and better-tolerated therapeutic strategies are a critical need.

Recently, we have demonstrated that **SAL** and semi-synthetic **SAL** derivatives obtained by chemical modification of the C1 carboxylate moiety inhibit the growth of culture-adapted bloodstream forms of *Trypanosoma brucei in vitro* at sub-micromolar concentration [20]. Interestingly, certain **SAL** analogues have been found to display enhanced trypanocidal activity compared to that of the parent ionophore with GI₅₀ values in the mid nanomolar range and MIC values below 1.0 μM. These anti-trypanosomal activities are within the range of the drugs used to treat African trypanosomiasis [20].

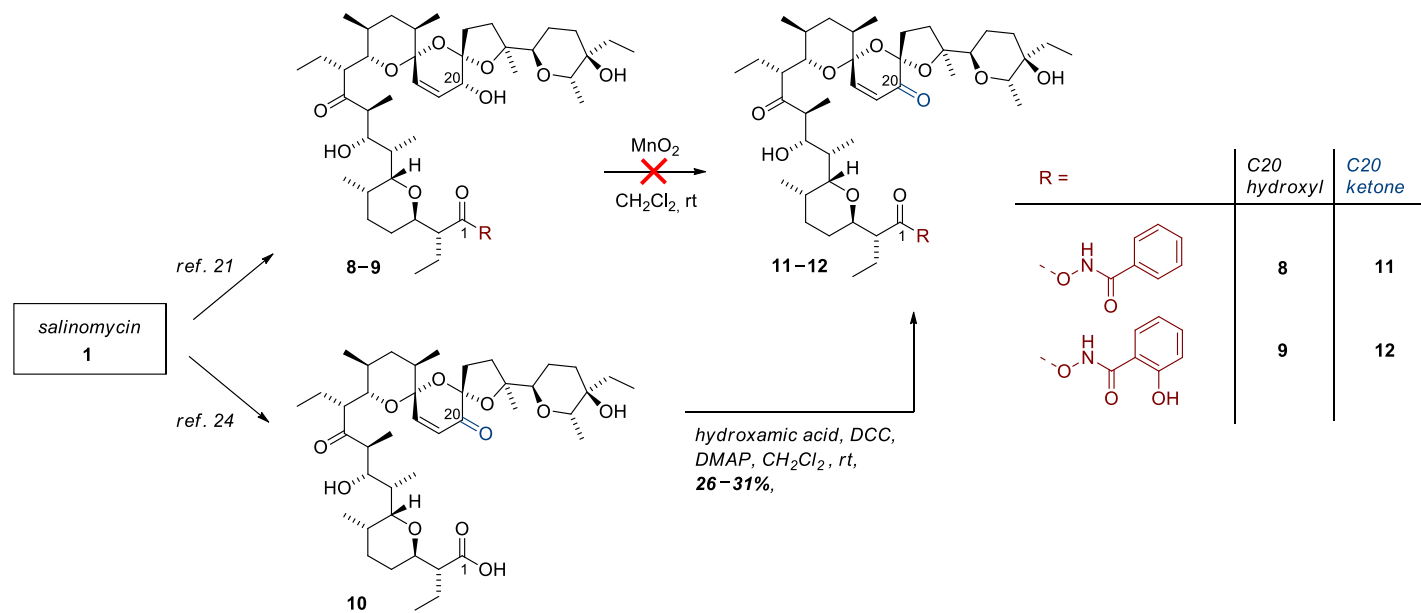
Besides C1 carboxylate moiety [20–23], the allylic C20 hydroxyl group of **SAL** has also been found to be an interesting site for chemical modification, as C20-*O*-acyl and C20-amine derivatives have been shown to have an improved biological activity profile compared to that of unmodified compound [24–25]. Recently, we have reported that doubly C1/C20 modified analogues of **SAL** display anti-cancer activity in the low μM range with low toxicity towards normal cells. In addition, these derivatives also showed good activity against a multi-drug resistant cancer cell line [26]. These findings indicate that multiple modifications of the **SAL** molecule may be also a promising synthetic strategy to improve the biological activity of this ionophore against *T. brucei*.

On the basis of our recent findings, we designed a completely novel class of multiply modified **SAL** derivatives by merging desirable structural features to generate promising anti-trypanosomal agents. In this context, methods for efficient synthetic access to novel double-modified analogues of C20-oxo and C20-propargylamine derivatives of a series of selected C1

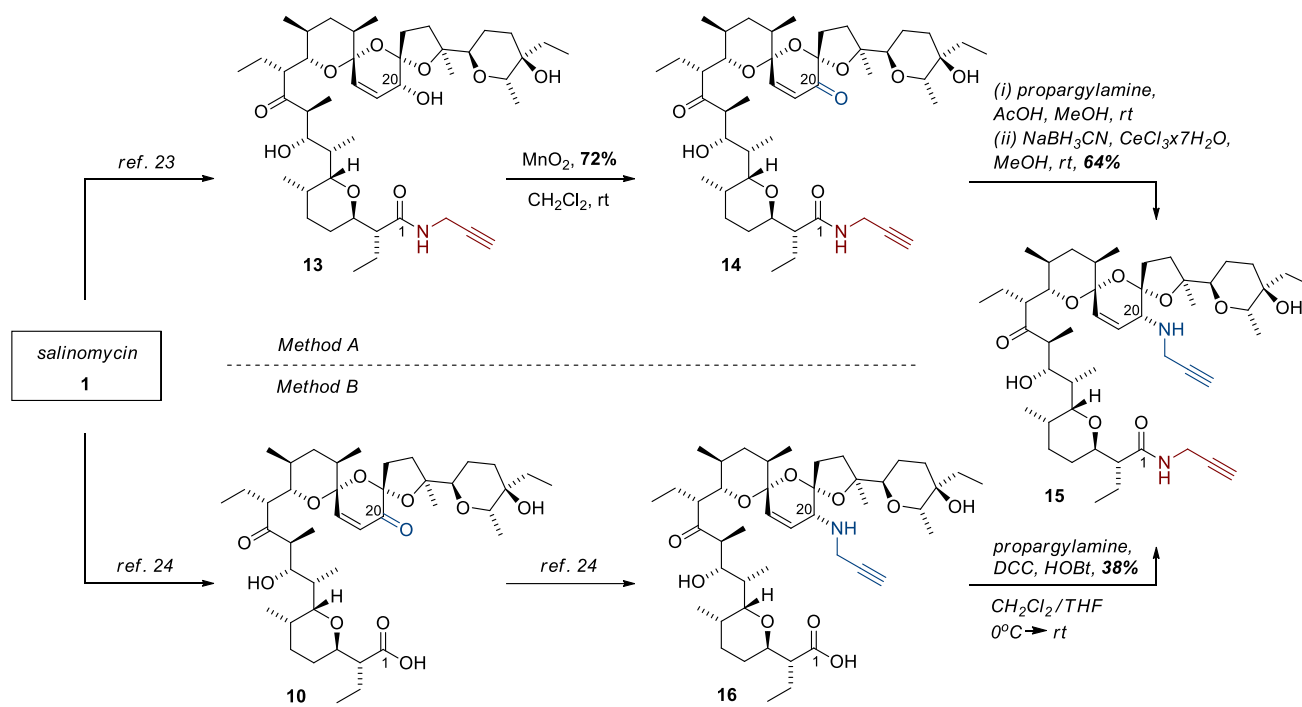
esters, amides and hybrids with hydroxamic acids are presented (**Schemes 1–3**). The newly synthesized compounds were evaluated *in vitro* for their trypanocidal and cytotoxic activity using bloodstream form of *T. brucei* and human myeloid HL-60 cells, respectively. The trypanocidal mechanism of the most active derivatives was investigated by swelling experiments.



Scheme 1. Synthesis of C1 esters and amides of C20-oxo-salinomycin.



Scheme 2. Synthesis of C1 conjugates of C20-oxo-salinomycin with hydroxamic acids.



Scheme 3. Synthesis of double-modified analogues **14** and **15**.

2. Results and discussion

2.1. Analogue design and synthesis

Firstly, to expand the library of novel doubly C1/C20 modified compounds, SAL analogues were designed on the basis of the most active C1 esters, amides and conjugates with hydroxamic acids obtained in previous studies [21–23], *i.e.* ester **2** and amide **4** (**Scheme 1**) as well as hybrids **8** and **9** (**Scheme 2**). Secondly, propargyl ester **3** (**Scheme 1**) and propargyl amide **13** (**Scheme 3**) were also included in our studies because of their structural similarity that might be of help in determination of structure-activity relationship (SAR). In addition, both structures were previously shown to display promising biological activity [23]. Thirdly, with respect to the modification of the C20 position, chemoselective oxidation of C20 hydroxyl was performed for all mentioned compounds to give access to six novel C20-oxo analogues (**Schemes 1–3**). Further stereoselective reductive amination of enone **14** (**Scheme 3**) was executed as well, as such a modification was expected to improve the biological activity of the resulting double-modified analogue (**Scheme 3**, compound **15**) [24]. Finally, to compare the trypanocidal activity of corresponding derivatives as well as to facilitate SAR analysis, both SAL precursors, C20 ketone **10** and C20 amine **16**, were also synthesized (**Scheme 2 and 3**) [24].

The allylic C20 hydroxyl group of the series of C1 esters and amides was chemoselectively oxidized to the corresponding C20 ketones with moderate to good yields (72–90%) using activated manganese(IV) oxide (**Scheme 1**, compounds **5–7** and **Scheme 3**, compound **14**) [24]. In all cases, full selectivity towards the C20 hydroxyl was observed. The synthesis of the double-modified analogues **11** and **12** (**Scheme 2**) was, however, slightly more challenging as the C20 hydroxyl group of the SAL hybrids with hydroxamic acids did not undergo oxidation under the reaction conditions. In order to obtain these compounds, it was

therefore necessary to synthesize C20-oxo-salinomycin **10** prior to its conjugation with benzhydroxamic acid or salicylhydroxamic acid (**Scheme 2**).

In 2017, Rodriguez and co-workers synthesized a series of C20-amine derivatives of **SAL** and found that the C20-propargylamine analogue (**Scheme 3**, compound **16**) was the most interesting one. The compound showed almost 10-times higher anti-proliferative activity against breast cancer stem cells than **SAL**, both *in vitro* and *in vivo*, with IC₅₀ value of ~100 nM whilst maintaining selectivity over control cells [24]. This finding inspired us to obtain a novel doubly modified analogue of **SAL** by transforming compound **14** to its corresponding C20-propargylamine **15** (**Scheme 3**, Method A), according to the protocol mentioned above [24]. In the first step of reductive amination, enone **14** reacted with propargylamine in the presence of acetic acid to form the imine *in situ*. Using the Luche reduction, the intermediate imine was then reduced by the slow addition of NaBH₃CN in the presence of CeCl₃, which resulted in the stereoselective formation of the novel double-modified derivative **15** with 64% yield (**Scheme 3**, Method A). Compound **15** was also obtained using the ‘reversed’ reaction sequence. Ketone **10** was converted into amine **16** [24], followed by an amidation reaction of C1 carboxyl moiety that resulted in the formation of **15** with 38% yield (**Scheme 3**, Method B). The overall yield of this transformation was however lower than the first one.

The purity and structure of the newly synthesized compounds were determined using scXRD, spectroscopic (FT-IR, NMR) and spectrometric (ESI MS) methods. The ¹H and ¹³C NMR spectra of selected **SAL** precursors and all novel double-modified analogues are included in **Supplementary Information**. The ¹⁹F NMR spectra of **5** and **7** that contain additional fluorine atoms in their structures are also included (see **Supplementary Information**). Briefly, in the ¹³C NMR spectra (in CD₂Cl₂ or in CDCl₃) of double-modified derivatives, the most

characteristic signal of α,β -unsaturated ketone at the C20 position was observed in a narrow range of 189.3–190.5 ppm. In the ^1H NMR spectrum of **15**, the characteristic signal of the alkynyl hydrogen of the C20 terminal alkyne moiety was observed at 2.21 (t, $J = 2.4$ Hz, 1H) ppm.

2.2. X-ray analysis

Structural data of SAL derivatives are very important to understand their biological properties, to determine SAR as well as related investigation. We have therefore characterized compounds **14** and **15** using the single-crystal X-ray diffraction (scXRD) method, and compared the obtained structures to the structure of the propargyl amide **13** described previously [27].

Single crystals of **14** (mp 115–119 °C) and **15** (mp 169–173 °C) were grown by crystallisation in acetonitrile solution. Compound **14** crystallized in the non-centrosymmetric space group $P2_1$ of the monoclinic system with one molecule in the asymmetric unit, while compound **15** crystallized in the non-centrosymmetric space group of the triclinic system with two molecules in the asymmetric unit. Crystal data and details of the refinement parameters are presented in **Table S1 (Supplementary Information)**. The asymmetric unit of the SAL derivatives **14** and **15** is illustrated in **Figure 1** and **Figure 2**, respectively.

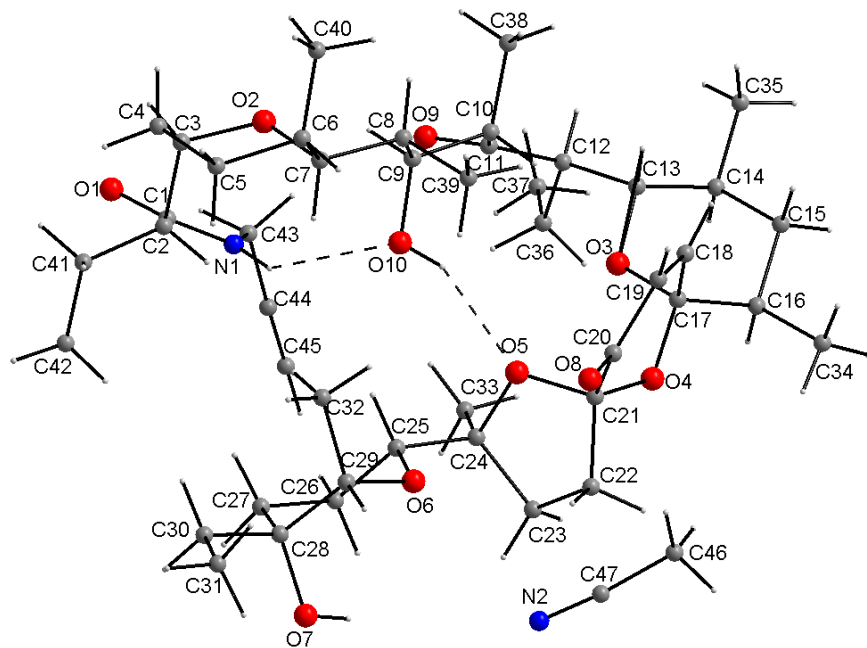


Figure 1. View of the asymmetric unit of **14**.

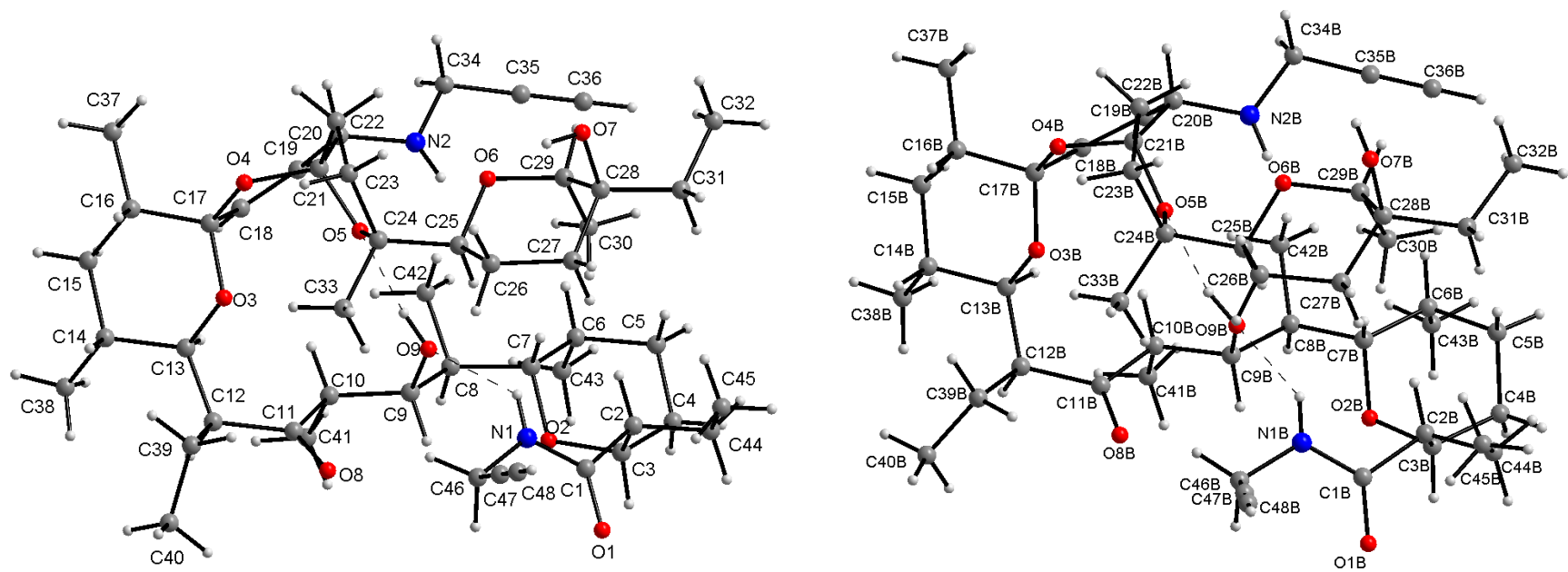


Figure 2. View of the asymmetric unit of **15** (Mol. 1 on the left, and Mol. 1B on the right).

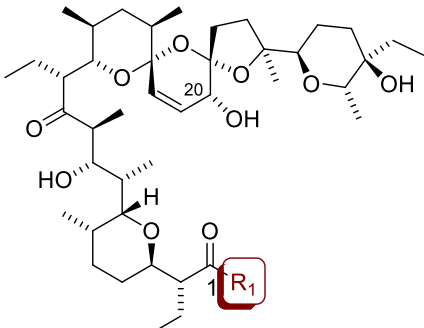
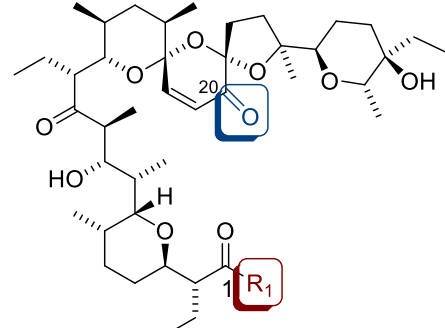
In the crystals, the molecules of both **SAL** derivatives exhibit pseudo-cyclic conformation. This conformation is stabilized by the O—H···O hydrogen bond formed by the hydroxyl group linked to C9 carbon atom and the O5 oxygen atom of the five-membered ring of the spiroketal system (**Supplementary Information, Table S2**) and, in addition, by an N—H···O hydrogen bond formed by the N—H of the amide group as a donor and the hydroxyl group as an acceptor that adds partly into the stabilization energy of the pseudo-cyclic conformation (**Figure 2**). Both independent molecules in the crystal of **15** (Mol. 1 and Mol. 1B) exhibit similar conformation (**Supplementary Information, Figure S1**), but differ from that of **14** due to the substitution effect at the C20 atom (**Supplementary Information, Figure S2**). The spiroketal system consists of two six-membered and one five-membered rings, in which the central rings are unsaturated. The arrangement of the atoms around the C17 and C21 heads is tetrahedral, so that the junctions between the five- and six-membered rings and between both six-membered rings are of the spiro type. The unsaturated six-membered ring with one double bond character (C18=C19), with a distance of 1.326(5) Å in **14** and 1.304(10) and 1.313(9) Å in the independent Mol. 1 and Mol. 1B molecules in **15**, has envelope conformation where C21 is out of the plane formed by the other ring atoms by 0.388(5) Å in **14**, and 0.508(8) and 0.486(8) Å in Mol. 1 and Mol. 1B in **15**, respectively. The five-membered ring of the spiro system exhibits twisted conformation with the C21 atom out of the mean plane defined by the other atoms of the ring by 0.443(5) Å in **14**, and 0.414(8) and 0.411(8) Å in Mol. 1 and Mol. 1B in **15**, respectively. All saturated six-membered rings exhibit chair conformation in both **14** and **15** structures. The X-ray crystallographic analysis confirmed the structural assignment (**Scheme 3**). The pseudo-cyclic conformation of **14** is quite similar to the conformation of **SAL** propargyl amide **13** (**Supplementary Information, Figure S3**), but the pseudo-cyclic conformation of **15** due to the

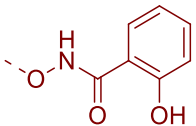

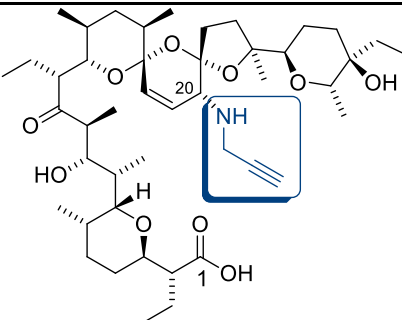
substitution effect at C20 is different to that of **SAL** propargyl amide **13** (**Supplementary Information, Figure S4**) [27].

2.3. *Anti-trypanosomal activity*

All **SAL** precursors and their newly synthesized double-modified derivatives were evaluated for their *in vitro* activity against bloodstream forms of *T. brucei* and human myeloid HL-60 cell using the resazurin cell viability assay [28,29]. All compounds showed a dose-dependent inhibitory effect on the growth of bloodstream-form trypanosomes (**Table 1**). Of the single-modified C1 esters and amides, only the benzhydroxamic acid conjugate **9** displayed a 6-fold enhanced trypanocidal activity compared to that of **SAL** with a 50% growth inhibition (GI_{50}) value of 0.035 μM . Both single-modified C20 analogues, C20-oxo and C20-propargylamine derivatives **10** and **16**, also exhibited increased anti-trypanosomal activity with similar GI_{50} values. Of the double-modified compounds, the benzhydroxamic acid and salicylhydroxamic acid conjugates **11** and **12** showed improved trypanocidal activity with GI_{50} values of 0.032 and 0.034 μM . However, their anti-trypanosomal activity was not better than that of their parent compound **10**.

Table 1. GI₅₀ values and ratios of SAL derivatives for *T. brucei* and HL-60 cells.

Single-modified salinomycin derivatives				Double-modified salinomycin derivatives				
								
No.	R ₁	<i>T. brucei</i>	HL-60	Selectivity	No.	<i>T. brucei</i>	HL-60	Selectivity
		GI ₅₀ (μM) ^a	GI ₅₀ (μM) ^a	GI ₅₀ ratio ^b		GI ₅₀ (μM) ^a	GI ₅₀ (μM) ^a	GI ₅₀ ratio ^b
1	-OH	0.21 ± 0.06	6.63 ± 3.23	31.6	10	0.037 ± 0.005	9.21 ± 4.25	252
2	-OCH ₂ CF ₃	2.90 ± 0.19	32.5 ± 0.8	11.2	5	3.01 ± 0.34	>100	>33.2
3	-OCH ₂ C≡CH	2.93 ± 0.14	30.0 ± 1.9	10.2	6	3.03 ± 0.06	29.6 ± 2.0	9.8
4	-NHCH ₂ CH ₂ C ₆ H ₄ F	2.87 ± 0.05	11.6 ± 1.6	4.0	7	2.99 ± 0.11	94.7 ± 7.7	31.7
8	-O-NH-C(=O)-C ₆ H ₅	0.17 ± 0.08	3.58 ± 0.98	21.1	11	0.032 ± 0.001	2.24 ± 0.87	70.0

9		0.035 ± 0.002	2.12 ± 0.31	60.6	12	0.034 ± 0.001	1.93 ± 0.77	56.8
13		3.06 ± 0.16	35.5 ± 0.1	11.6	14	3.18 ± 0.08	38.6 ± 7.6	12.1
16		0.035 ± 0.005	10.5 ± 6.5	300	15	3.04 ± 0.13	38.9 ± 2.5	12.8
Suramin ^c		0.032 ± 0.003	>100	>3125				

^a Data shown are mean values \pm SD of three independent experiments; ^b GI₅₀ ratio = GI₅₀(HL-60)/GI₅₀(*T. brucei*); ^c Reference control.

Most derivatives showed lower cytotoxic activity against HL-60 cells than **SAL** (**Table 1**). However, compounds **9**, **11** and **12** displayed increased cytotoxicities. As the single modified C20 derivatives were less cytotoxic towards HL-60 cells, their selectivity index (GI_{50} ratio of cytotoxic to trypanocidal activity) was 8–9 fold increased relative to that of **SAL** (**Table 1**).

Noteworthy is the finding that all five compounds (**9–12** and **16**) with increased trypanocidal activity displayed GI_{50} values similar to the GI_{50} value of suramin, one of the drugs used in the treatment of sleeping sickness (**Table 1**). However, as suramin is nontoxic to HL-60 cells, the selectivity indices of the derivatives were less favorable than the GI_{50} ratio of suramin,

It has been shown that **SAL** derivatives with enhanced trypanocidal activity display increased ionophoretic activity when compared to that of the unmodified parent compound [20]. Therefore, we wanted to check whether the enhanced anti-trypanosomal activity of compounds **9–12** and **16** was also due to increased ionophoresis. Changes in cell volume were determined by swelling experiments using the light scattering method previously described [20]. Only the C20-oxo derivative **10** produced an increased swelling in bloodstream-form trypanosomes while the C20-propargylamine derivative **16** generated a similar swelling in the parasites as the parent compound (**Figure 3**). The other three compounds displayed lower (**9**) and much lower (**11** and **12**) ionophoresis (**Figure 3**). Based on their low GI_{50} values (0.032–0.035 μ M, **Table 1**) in connection with their low ionophoretic activity, the trypanocidal activity of compounds **9**, **11** and **12** may be not only due to their ionophoretic properties but probably to other mechanisms of toxic action.

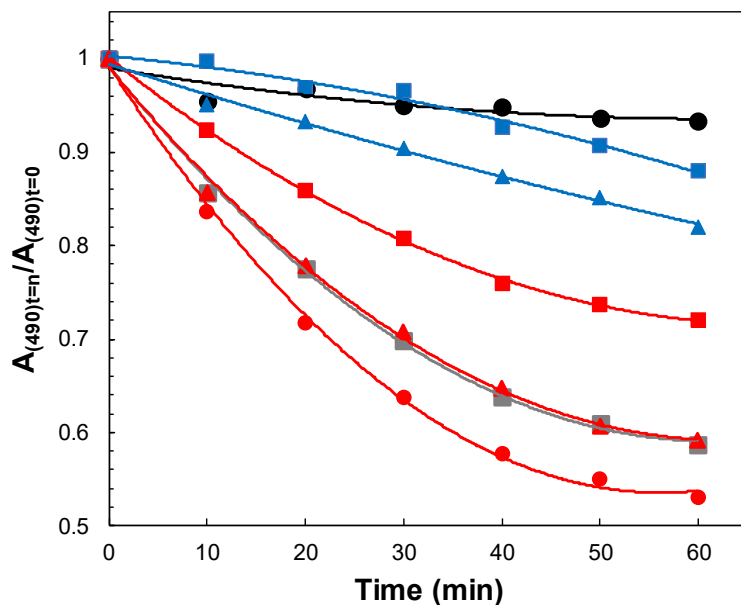


Figure 3. Effect of SAL derivatives on the cell volume of bloodstream forms of *T. brucei*. Trypanosomes (5×10^7 cells ml^{-1}) were incubated with $100 \mu\text{M}$ ionophore in Baltz medium in the presence of 0.9% DMSO. Every 10 min, the absorbance at 490 nm was measured. Black circles, DMSO control; grey squares, SAL control; red, single-modified derivatives (squares, **9**; circles, **10**; triangles, **16**); blue, double-modified derivatives (squares, **11**; triangles, **12**). Note that a decrease in absorbance corresponds to an increase in cell volume. For clarity, only mean values of three experiments are shown. The standard deviations ranged from 0.1 to 12.1 percentage points.

Evaluation of the trypanocidal activity of the new SAL derivatives has shown that modification of the C20 hydroxyl group to its ketone and propargylamine analogues **10** and **16** gave compounds with increased anti-trypansomal activity. Further modification of **10** or **16** at their C1 position did not lead to an additional increase in trypanocidal activity. The anti-trypansomal activity of the double-modified compounds was either decreased (**5–7**, **14** and **15**) or stayed the same (**11** and **12**). As the cytotoxic activity of the double-modified derivatives paralleled their trypanocidal activity, their selectivity was not much different from that of SAL.

3. Conclusions

In summary, a series of novel double-modified **SAL** analogues derivatized at their C1/C20 positions was devised. All newly designed compounds were synthesized in moderate to good yields. Of advantage were the straightforward protocols that allowed simple reaction workup and convenient isolation of the analogues.

X-ray single crystal analyses of both **SAL** derivatives **14** and **15** showed pseudo-cyclic conformation of the skeletal molecules that were stabilized by the intramolecular O—H···O and N—H···O hydrogen bonds. A slight differences in the conformation between these **SAL** derivatives resulted from the substitution effect at the carbon atom C20 in the unsaturated six-membered ring.

With respect to trypanocidal activity, double-modified derivatives showed at best anti-trypanosomal activity similar to that of their single-modified starting molecules, wherein compounds **11** and **12** seem to be the most promising ones in this group. However, their selectivity was not significantly improved. The most trypanocidal and selective compounds were the **SAL** derivatives **10** and **16** that were single-modified at their C20 position. These two analogues match the activity criteria for drug candidates for African trypanosomiasis ($GI_{50} < 1 \mu\text{M}$; selectivity > 100).

4. Experimental

4.1. General procedures

All precursors (except for hydroxamic acids, see section 4.2 for details) and all solvents were obtained from Merck or Trimen Chemicals S.A. (Poland), and were used as received without further purification. CD_2Cl_2 and CDCl_3 spectral grade solvents were stored over 3Å molecular sieves for several days. All manipulations were carried out under nitrogen atmosphere

in oven-dried glassware. Reaction mixtures were stirred using teflon-coated magnetic stir bars. Reaction mixtures were monitored by thin layer chromatography (TLC) using aluminum-backed plates (Merck 60F254). TLC plates were visualized by UV-light (254 nm), followed by treatment with phosphomolybdic acid (PMA, 5% in absolute EtOH) and gentle heating. Products of the reactions were purified using CombiFlash® Rf+ Lumen Flash Chromatography System (Teledyne Isco) with integrated ELS and UV detectors. All solvents used in flash chromatography were of HPLC grade (Merck) and were used as received. Solvents were removed using a rotary evaporator.

NMR spectra were recorded on a Varian 400 (^1H NMR at 403 MHz, ^{13}C NMR at 101 MHz, and ^{19}F NMR at 379 or 282 MHz) magnetic resonance spectrometer. ^1H NMR spectra are reported in chemical shifts downfield from TMS using the respective residual solvent peak as internal standard (CD_2Cl_2 δ 5.32 ppm and CDCl_3 δ 7.26 ppm). ^1H NMR spectra are reported as follows: chemical shift (δ , ppm), multiplicity (s = singlet, d = doublet, t = triplet, q = quartet, hept = heptet, dd = doublet of doublets, dt = doublet of triplets, dq = doublet of quartets, ddd = doublet of doublet of doublets, ddt = doublet of doublet of triplets, dtd = doublet of triplet of doublets, td = triplet of doublets, tdd = triplet of doublet of doublets, qd = quartet of doublets, m = multiplet), coupling constant(s) in Hz, and integration. Significant peaks are reported within the overlapping ~ 2.00 – 0.50 ppm region of the ^1H NMR spectra. ^{13}C NMR spectra are reported in chemical shifts downfield from TMS using the respective residual solvent peak as internal standard (CD_2Cl_2 δ 53.84 ppm and CDCl_3 δ 77.16 ppm). ^{19}F NMR spectra are reported in chemical shifts upfield from TMS using CFCl_3 as internal standard. Line broadening parameters were 0.5 or 1.0 Hz, while the error of chemical shift value was 0.1 ppm.

Infrared spectra in the mid infrared region were recorded in KBr tablets on an IFS 113v FT-IR spectrophotometer (Bruker) equipped with a DTGS detector, and are reported as follows: wavenumbers (cm^{-1}), description (w = weak, m = medium, s = strong, br = broad). The spectra were taken on resolution 2 cm^{-1} , NSS = 64. The Happ-Genzel apodization function was used.

Electrospray ionization (ESI) mass spectra were recorded on a Waters/Micromass ZQ mass spectrometer (Waters Alliance) equipped with a Harvard syringe pump. Samples were prepared in dry acetonitrile, and were infused into the ESI source using a Harvard pump at a flow rate of 20 ml min^{-1} . The ESI source potentials were: capillary 3 kV, lens 0.5 kV, and extractor 4 V. Standard ESI mass spectra were recorded at the cone voltages of 10 and 30 V. The source temperature was $120 \text{ }^\circ\text{C}$ and the desolvation temperature was $300 \text{ }^\circ\text{C}$. Nitrogen was used as the nebulizing and desolvation gas at flow-rates of $100 \text{ dm}^3 \text{ h}^{-1}$. Mass spectra were acquired in the positive ion detection mode with unit mass resolution at a step of 1 m/z unit. The mass range for ESI experiments was from $m/z = 300$ to $m/z = 1100$.

4.2. Synthesis

Salinomycin sodium salt was isolated from commercially available veterinary premix SACOX[®] following acidic extraction, using the procedure described by us previously [22–23]. Briefly, isolated sodium salt of salinomycin was dissolved in CH_2Cl_2 and stirred vigorously with a layer of aqueous sulphuric acid (pH = 1.0). The organic layer containing **SAL** was washed with distilled water, and then CH_2Cl_2 was evaporated under reduced pressure to dryness giving **SAL** as a clear oil. After 3-times repeated evaporation with *n*-pentane this oil was transformed to white amorphous solid. The spectroscopic data of **SAL** were in agreement with previously published data [30].

Hydroxamic acid precursors were obtained from the corresponding carboxylic acids according to the procedure published by Jirgensons *et al.* [31], and used then for the synthesis of **SAL** conjugates following the procedure described by Wu *et al.* [21]. All **SAL** C1 esters and amides were prepared using the procedures described by us previously [22–23]. Compounds **10** and **16** were prepared following the procedures described by Rodriguez *et al.* [24]. The NMR data of all the compounds were in good agreement with those found in the reference literature.

4.2.1. General procedure for preparation of novel C20-oxo derivatives of salinomycin esters and amides (analogues **5–7** and **14**)

To a stirred solution of **SAL** ester or amide (1.0 equiv.) in CH₂Cl₂ at room temperature, activated manganese(IV) oxide (20.0 equiv.) was added in one portion. The resulting black suspension was stirred vigorously for 3 days, and then filtrated over celite. The filtrate was diluted with CH₂Cl₂ and washed with an aqueous solution of H₂SO₄ (pH = 1.0) and distilled water. The organic layer was separated and concentrated under reduced pressure to give a colorless oil. Purification on silica gel using the CombiFlash system (EtOAc/*n*-hexane) gave the pure products of the reactions for **5–7** and **14** (72–90% yield) as colorless oils. After 3-times repeated evaporation with *n*-pentane the oils were transformed to white amorphous solids.

4.2.1.1. 2,2,2-trifluoroethyl ester of C20-oxo-salinomycin **5**

Yield: 760 mg, 88%. Isolated as a white amorphous solid, >95% pure by NMR and a single spot by TLC; R_f: 0.59 in 33% EtOAc/*n*-hexane. UV-active and strains green with PMA; ¹H NMR (403 MHz, CDCl₃) δ 7.24 (d, *J* = 10.8 Hz, 1H), 6.23 (d, *J* = 10.8 Hz, 1H), 4.75 (ddd, *J* = 17.3, 12.9, 8.6 Hz, 1H), 4.65 (ddd, *J* = 17.3, 13.0, 8.7 Hz, 1H), 4.06 (dd, *J* = 10.9, 5.5 Hz, 1H),

3.88 (ddd, $J = 10.1, 5.3, 1.0$ Hz, 1H), 3.76 (q, $J = 6.9$ Hz, 1H), 3.64 (dd, $J = 10.1, 3.9$ Hz, 1H), 3.57 (dd, $J = 9.8, 1.9$ Hz, 1H), 3.48 (s, 1H), 3.42–3.34 (m, 1H), 3.10 (td, $J = 10.9, 4.4$ Hz, 1H), 2.97 (dq, $J = 10.1, 7.1$ Hz, 1H), 2.78–2.55 (m, 4H), 2.19–2.03 (m, 2H), 2.02–0.66 (m, 50H) ppm; ^{13}C NMR (101 MHz, CDCl_3) δ 214.4, 190.4, 173.9, 143.6, 127.3, 124.6, 121.8, 105.4, 97.5, 88.6, 78.5, 77.1, 74.5, 72.0, 71.9, 71.0, 70.0, 60.8, 60.4, 57.0, 48.8, 47.2, 39.7, 39.0, 36.3, 34.2, 34.1, 34.0, 30.4, 29.1, 28.0, 26.2, 22.7, 22.5, 20.7, 19.7, 18.9, 17.5, 15.8, 14.3, 13.9, 12.0, 11.5, 11.0, 7.2, 6.4 ppm; ^{19}F NMR (282 MHz, chloroform-*d*) δ –73.97 ppm; FT-IR (KBr tablet): 3581 (br, m), 3458 (br, m), 2967 (s), 2939 (s), 2882 (s), 1755 (s), 1736 (m), 1697 (s), 1461 (s), 1446 (s), 1442 (s), 1406 cm^{-1} ; ESI MS (m/z): $[\text{M}+\text{Na}]^+$ Calcd for $\text{C}_{44}\text{H}_{69}\text{F}_3\text{NaO}_{11}$ 853; Found 853.

4.2.1.2. Propargyl ester of C20-oxo-salinomycin 6

Yield: 380 mg, 79%. Isolated as a white amorphous solid, >95% pure by NMR and a single spot by TLC; R_f : 0.64 in 33% EtOAc/*n*-hexane. UV-active and strains green with PMA; ^1H NMR (403 MHz, CD_2Cl_2) δ 7.23 (d, $J = 10.8$ Hz, 1H), 6.19 (d, $J = 10.8$ Hz, 1H), 4.82 (qd, $J = 15.8, 2.5$ Hz, 2H), 3.97 (dd, $J = 11.0, 5.5$ Hz, 1H), 3.84 (ddd, $J = 10.1, 5.0, 1.0$ Hz, 1H), 3.72 (q, $J = 6.8$ Hz, 1H), 3.65 (dd, $J = 10.1, 3.4$ Hz, 1H), 3.54 (dd, $J = 9.8, 1.9$ Hz, 1H), 3.41–3.32 (m, 1H), 3.02 (td, $J = 10.7, 4.7$ Hz, 1H), 2.93 (dq, $J = 10.1, 7.1$ Hz, 1H), 2.68–2.63 (m, 2H), 2.63–2.51 (m, 2H), 2.13–1.98 (m, 2H), 1.96–0.61 (m, 52H) ppm; ^{13}C NMR (101 MHz, CD_2Cl_2) δ 214.5, 190.5, 175.2, 143.9, 127.6, 105.8, 97.9, 89.1, 79.0, 78.6, 77.5, 75.1, 72.6, 72.2, 71.1, 70.4, 57.0, 52.7, 49.0, 47.5, 40.2, 39.2, 36.7, 34.6, 34.4, 34.2, 30.8, 29.6, 28.5, 26.6, 23.3, 23.1, 21.1, 20.1, 18.7, 17.7, 15.9, 14.5, 14.2, 12.6, 11.8, 11.2, 7.5, 6.6 ppm, one signal overlapped; FT-IR (KBr tablet): 3541 (br, m), 3469 (br, m), 3313 (m), 2966 (s), 2938 (s), 2877 (s), 2124 (w), 1745

(s), 1724 (s), 1700 (s), 1460 (s), 1444 (s), 1405 (s) cm^{-1} ; ESI MS (m/z): $[\text{M}+\text{Na}]^+$ Calcd for $\text{C}_{45}\text{H}_{70}\text{NaO}_{11}$ 810; Found 810.

4.2.1.3. 4-fluorophenethyl amide of C20-oxo-salinomycin 7

Yield: 320 mg, 90%. Isolated as a white amorphous solid, >95% pure by NMR and a single spot by TLC; R_f : 0.46 in 50% EtOAc/*n*-hexane. UV-active and strains green with PMA; ^1H NMR (403 MHz, CDCl_3) δ 7.29–7.22 (m, 3H), 7.00–6.91 (m, 2H), 6.32 (t, $J = 5.8$ Hz, 1H), 6.23 (d, $J = 10.7$ Hz, 1H), 4.03 (dd, $J = 9.7, 3.2$ Hz, 1H), 3.85 (dd, $J = 10.8, 4.2$ Hz, 1H), 3.78–3.60 (m, 4H), 3.59–3.50 (m, 1H), 3.51–3.47 (m, 1H), 3.35 (dd, $J = 11.0, 2.1$ Hz, 1H), 3.14 (s, 1H), 2.93–2.80 (m, 3H), 2.73 (td, $J = 10.7, 4.4$ Hz, 1H), 2.70–2.65 (m, 1H), 2.60 (ddd, $J = 11.7, 7.2, 4.0$ Hz, 1H), 2.14–0.56 (m, 53H) ppm; ^{13}C NMR (101 MHz, CDCl_3) δ 214.1, 190.1, 175.1, 162.7, 160.3, 143.4, 135.20, 135.17, 130.34, 130.26, 127.6, 115.1, 114.9, 105.7, 97.4, 89.0, 78.5, 77.4, 75.3, 72.5, 71.4, 70.8, 70.2, 55.3, 49.0, 46.3, 40.5, 39.7, 38.7, 36.4, 35.0, 34.4, 34.1, 33.6, 30.4, 29.1, 28.3, 26.5, 23.5, 22.6, 20.6, 17.6, 17.5, 15.8, 14.4, 12.6, 11.7, 11.5, 7.6, 6.5 ppm; FT-IR (KBr tablet): 3505 (m), 3424 (br, m), 3359 (m), 3057 (w), 2965 (s), 2931 (s), 2876 (s), 1711 (br, s), 1709 (br, s), 1659 (s), 1602 (m), 1524 (s), 1512 (s), 1466 (s), 1456 (s), 1440 (s), 1402 (s) cm^{-1} ; ESI MS (m/z): $[\text{M}+\text{Na}]^+$ Calcd for $\text{C}_{50}\text{H}_{76}\text{FNNaO}_{10}$ 893; Found 893.

4.2.1.4. Propargyl amide of C20-oxo-salinomycin 14

Yield: 600 mg, 72%. Isolated as a white amorphous solid, >95% pure by NMR and a single spot by TLC; R_f : 0.60 in 50% EtOAc/*n*-hexane. UV-active and strains green with PMA; ^1H NMR (403 MHz, CD_2Cl_2) δ 7.29 (d, $J = 10.8$ Hz, 1H), 7.19–7.08 (m, 1H), 6.20 (d, $J = 10.7$ Hz, 1H), 4.27 (ddd, $J = 17.6, 6.3, 2.5$ Hz, 1H), 4.03 (ddd, $J = 17.7, 5.0, 2.5$ Hz, 1H), 3.97–3.84

(m, 2H), 3.81 (q, $J = 6.9$ Hz, 1H), 3.76–3.65 (m, 2H), 3.62 (dd, $J = 9.8, 2.0$ Hz, 1H), 3.39–3.28 (m, 1H), 3.20 (d, $J = 3.8$ Hz, 1H), 2.85–2.66 (m, 2H), 2.62 (dt, $J = 8.8, 3.0$ Hz, 1H), 2.58–2.47 (m, 1H), 2.17 (t, $J = 2.5$ Hz, 1H), 2.07–0.53 (m, 53H) ppm; ^{13}C NMR (101 MHz, CD_2Cl_2) δ 214.1, 190.0, 175.1, 143.6, 128.4, 106.4, 97.8, 89.7, 81.8, 79.7, 78.2, 75.5, 73.3, 71.7, 71.2, 70.2, 70.1, 54.3, 48.4, 46.3, 40.1, 38.6, 36.8, 35.0, 34.4, 33.2, 30.8, 29.4, 28.8, 26.9, 24.9, 23.0, 20.9, 20.5, 17.3, 17.1, 15.9, 14.7, 14.6, 13.6, 11.8, 11.4, 8.0, 6.9 ppm, one signal overlapped; FT-IR (KBr tablet): 3472 (m), 3430 (br, m), 3338 (m), 3319 (m), 2966 (s), 2934 (s), 2878 (s), 2128 (w), 1703 (br, s), 1653 (s), 1531 (s), 1460 (s), 1443 (m), 1437 (m) cm^{-1} ; ESI MS (m/z): $[\text{M}+\text{Na}]^+$ Calcd for $\text{C}_{45}\text{H}_{71}\text{NNaO}_{10}$ 808; Found 808.

4.2.2. General procedure for preparation of novel conjugates of C20-oxo-salinomycin with hydroxamic acids (analogues **11** and **12**)

To a stirred solution of C20-oxo-salinomycin **10** (1.0 equiv.) in anhydrous CH_2Cl_2 at room temperature, 1,3-dicyclohexylcarbodiimide (2.0 equiv.) and an excess of 4-dimethylaminopyridine were added, followed by addition of the corresponding hydroxamic acid (5.0 equiv.) in one portion. The resulting pale yellow solution was stirred for 24 hours, and then the organic solvents were evaporated under reduced pressure to dryness. The yellow residue was re-suspended in CH_2Cl_2 and filtered to remove the 1,3-dicyclohexylurea by-product. The filtrate was evaporated under reduced pressure and purified on silica gel using the CombiFlash system (EtOAc/ n -hexane) to give the pure products of the reaction for **11** and **12** (26–31% yield) as clear oils. After 3-times repeated evaporation with n -pentane the oils were transformed to white amorphous solids.

4.2.2.1. Benzhydroxamic acid conjugate of C20-oxo-salinomycin **11**

Yield: 323 mg, 31%. Isolated as a white amorphous solid, >95% pure by NMR and a single spot by TLC; R_f : 0.78 in 50% EtOAc/*n*-hexane. UV-active and strains green with PMA; ^1H NMR (401 MHz, CD_2Cl_2) δ 11.05 (s, 1H), 8.19–8.05 (m, 2H), 7.59–7.49 (m, 1H), 7.48–7.38 (m, 2H), 7.23 (d, $J = 10.8$ Hz, 1H), 6.20 (d, $J = 10.8$ Hz, 1H), 4.05–3.91 (m, 2H), 3.84–3.74 (m, 2H), 3.69 (dd, $J = 9.7, 1.9$ Hz, 1H), 3.30 (dd, $J = 11.5, 2.3$ Hz, 1H), 3.15 (ddd, $J = 11.0, 8.7, 6.1$ Hz, 1H), 2.94–2.82 (m, 2H), 2.64–2.51 (m, 2H), 2.38 (d, $J = 5.3$ Hz, 1H), 2.04–1.96 (m, 1H), 1.95–0.50 (m, 52H) ppm; ^{13}C NMR (101 MHz, CD_2Cl_2) δ 216.6, 189.3, 173.9, 165.6, 142.5, 132.4, 131.6, 128.7, 128.5, 128.3, 105.9, 97.9, 90.2, 80.4, 76.8, 75.0, 72.8, 72.7, 70.9, 69.5, 54.1, 46.9, 46.7, 40.2, 38.3, 36.5, 34.6, 33.0, 32.7, 31.3, 29.9, 28.7, 26.8, 25.4, 23.5, 21.3, 20.3, 17.1, 16.6, 15.9, 14.9, 14.5, 14.2, 11.9, 11.2, 7.8, 6.8 ppm; FT-IR (KBr tablet): 3570 (m), 3501 (br, m), 3321 (br, m), 3064 (m), 2965 (s), 2938 (s), 2879 (s), 1781 (s), 1702 (br, s), 1637 (m), 1602 (m), 1583 (m), 1542 (m), 1502 (m), 1462 (s), 1446 (s), cm^{-1} ; ESI MS (m/z): $[\text{M}+\text{Na}]^+$ Calcd for $\text{C}_{49}\text{H}_{73}\text{NNaO}_{12}$ 891; Found 891.

4.2.2.2. Salicylhydroxamic acid conjugate of C20-oxo-salinomycin **12**

Yield: 130 mg, 26%. Isolated as a white amorphous solid, >95% pure by NMR and a single spot by TLC; R_f : 0.35 in 50% EtOAc/*n*-hexane. UV-active and strains green with PMA; ^1H NMR (401 MHz, CD_2Cl_2) δ 11.71 (s, 1H), 11.25 (s, 1H), 8.25 (dd, $J = 8.0, 1.4$ Hz, 1H), 7.43 (ddd, $J = 8.6, 7.3, 1.5$ Hz, 1H), 7.26 (d, $J = 10.8$ Hz, 1H), 6.95 (dd, $J = 8.4, 1.0$ Hz, 1H), 6.90–6.83 (m, 1H), 6.22 (d, $J = 10.8$ Hz, 1H), 4.06–3.97 (m, 2H), 3.86 (dd, $J = 10.1, 2.8$ Hz, 1H), 3.77 (q, $J = 6.9$ Hz, 1H), 3.71 (dd, $J = 9.6, 1.9$ Hz, 1H), 3.30 (dd, $J = 11.6, 2.3$ Hz, 1H), 3.18 (ddd, $J = 11.0, 7.7, 6.9$ Hz, 1H), 2.90 (dq, $J = 9.5, 7.4$ Hz, 2H), 2.66 (dt, $J = 9.1, 2.4$ Hz, 1H), 2.64–2.51

(m, 1H), 2.40 (d, $J = 5.7$ Hz, 1H), 2.10–0.50 (m, 53H) ppm; ^{13}C NMR (101 MHz, CD_2Cl_2) δ 217.2, 189.4, 173.8, 169.0, 162.1, 142.7, 135.2, 128.8, 127.9, 119.2, 118.5, 112.4, 106.1, 98.1, 90.6, 80.6, 77.0, 75.2, 73.2, 72.9, 71.1, 69.6, 54.2, 47.0, 46.7, 40.4, 38.5, 36.7, 34.9, 33.0, 32.9, 31.4, 30.1, 28.8, 27.0, 25.9, 23.7, 21.7, 20.5, 17.4, 16.6, 16.1, 15.2, 14.60, 14.58, 12.0, 11.4, 8.0, 7.0 ppm; FT-IR (KBr tablet): 3567 (br, m), 3301 (m), 2967 (s), 2939 (s), 2880 (s), 1788 (s), 1702 (br, s), 1655 (s), 1610 (s), 1588 (m), 1508 (s), 1484 (s), 1461 (s), 1448 (s) cm^{-1} ; ESI MS (m/z): $[\text{M}+\text{Na}]^+$ Calcd for $\text{C}_{49}\text{H}_{73}\text{NNaO}_{13}$ 907; Found 907.

4.2.3. General procedure for preparation of novel salinomycin C20-propargylamine **15**

Method A: To a stirred solution of ketone **14** (1.0 equiv.) in MeOH at room temperature, propargylamine (10.0 equiv.) was added, followed by addition of a small portion of acetic acid. The resulting yellow solution was stirred for 1 hour at room temperature prior to the addition of $\text{CeCl}_3 \cdot 7\text{H}_2\text{O}$ (1.0 equiv.), followed by the dropwise addition of a solution of NaBH_3CN (2.0 equiv.) in MeOH over 12 hours using a dropping funnel. Organic solvent was then evaporated to dryness under reduced pressure to give a yellow oil. The yellow residue was re-dissolved in CH_2Cl_2 , and washed twice with an aqueous solution of H_2SO_4 (pH = 1.0) and finally with distilled water. The organic layer was separated, concentrated under reduced pressure and purified on silica gel using the CombiFlash system (50% EtOAc/ CHCl_3) to give the pure product **15** (64% yield) as a colorless oil. After 3-times repeated evaporation with *n*-pentane the oil was transformed to a white amorphous solid.

Method B: A solution of amine **16** (1.0 equiv.), 1,3-dicyclohexylcarbodiimide (1.2 equiv.) and propargylamine (2.0 equiv.) in CH_2Cl_2 was mixed with 1-hydroxybenzotriazole hydrate (0.5 equiv.) in THF, and stirred at 0 °C for 1 hour. Then, the reaction mixture was stirred

at room temperature for further 24 hours. Afterwards, the organic solvents were evaporated under reduced pressure to dryness. The yellow residue was re-suspended in CH₂Cl₂ and filtered to remove the 1,3-dicyclohexylurea by-product. The filtrate was evaporated under reduced pressure and purified on silica gel using the CombiFlash system (50% EtOAc/CHCl₃) to give the pure product **15** (38% yield) as a colorless oil. After 3-times repeated evaporation with *n*-pentane the oil was transformed to white amorphous solid.

4.2.3.1. Propargyl amide of C20-propargylaminosalinomycin **15**

Yield: 230 mg, 64%. Isolated as a white amorphous solid, >95% pure by NMR and a single spot by TLC; R_f: 0.41 in 50% EtOAc/*n*-hexane. Strains green with PMA; ¹H NMR (400 MHz, CD₂Cl₂) δ 7.27 (t, *J* = 5.5 Hz, 1H), 6.10 (dd, *J* = 10.7, 2.2 Hz, 1H), 5.95 (dd, *J* = 10.7, 1.6 Hz, 1H), 4.37 (ddd, *J* = 17.6, 5.9, 2.5 Hz, 1H), 4.18 (ddd, *J* = 17.6, 5.3, 2.5 Hz, 1H), 4.07 (d, *J* = 9.6 Hz, 1H), 3.93–3.85 (m, 1H), 3.80 (dd, *J* = 13.7, 6.8 Hz, 1H), 3.68 (ddd, *J* = 20.1, 10.0, 2.3 Hz, 2H), 3.58 (dd, *J* = 11.8, 2.2 Hz, 1H), 3.46 (qd, *J* = 16.8, 2.4 Hz, 2H), 3.19 (t, *J* = 1.8 Hz, 1H), 3.00–2.82 (m, 2H), 2.70–2.56 (m, 2H), 2.54–2.47 (m, 1H), 2.24 (ddd, *J* = 11.5, 8.2, 6.1 Hz, 2H), 2.14–2.03 (m, 2H), 1.92–0.54 (m, 53H) ppm; ¹³C NMR (101 MHz, CD₂Cl₂) δ 212.9, 175.3, 132.4, 119.9, 106.7, 98.7, 89.0, 82.8, 82.2, 79.5, 77.3, 75.7, 74.6, 71.3, 71.1, 71.0, 69.4, 69.0, 55.5, 53.8, 48.2, 46.9, 40.8, 38.7, 37.9, 37.6, 36.6, 32.9, 30.9, 30.8, 29.6, 28.9, 28.6, 27.1, 25.9, 22.43, 22.40, 20.7, 17.6, 17.4, 15.9, 14.8, 14.6, 14.5, 12.0, 11.7, 8.2, 6.6 ppm; FT-IR (KBr tablet): 3484 (s), 3434 (br, m), 3312 (s), 2963 (s), 2935 (s), 2877 (s), 1712 (s), 1668 (s), 1524 (s), 1459 (s), 1419 (m), 1403 (m) cm⁻¹; ESI MS (*m/z*): [M+H]⁺ Calcd for C₄₈H₇₇N₂O₉ 826; Found 826.

4.3. X-ray measurements

X-ray data collection for colorless single crystals of **14** and **15** was performed on a four-circle KUMA KM-4 diffractometer equipped with a two-dimensional CCD area detector. The graphite monochromatized MoK α radiation ($\lambda=0.71973$ Å) and the ω scan technique ($\Delta\omega=1^\circ$) were used for data collection. Data collection and reduction along with absorption correction were performed using CrysAlis software package [32]. The structure was solved by direct methods using the *SHELXT* program revealing positions of almost all non-hydrogen atoms. The remaining atoms were located from subsequent difference Fourier syntheses. The structure was refined using SHELXL-2014 [33] with the anisotropic thermal displacement parameters. The hydrogen atoms of the aromatic ring were refined with riding model. Visualization of the structures was made with the Diamond 3.0 program [34]. Details of the data collection parameters, crystallographic data and final agreement parameters are given in **Table S1 (Supplementary Information)**. Hydrogen bonding geometry is collected in **Table S2 (Supplementary Information)**.

4.4. In vitro biological studies

4.4.1. Cell Culture

Bloodstream form of *T. brucei* 427-221a [35] and human myeloid HL-60 cells [36] were cultured in Bartz medium [37] supplemented with 16.7% heat-inactivated bovine serum. All cultures were maintained at 37 °C in a humidified atmosphere containing 5% carbon dioxide.

4.4.2. Trypanocidal and cytotoxic assays

Toxicity assays were performed as previously described [28,29]. In brief, trypanosomes and HL-60 cells were seeded at an initial cell density of $1 \times 10^4 \text{ ml}^{-1}$ and $5 \times 10^4 \text{ ml}^{-1}$, respectively, in 96-well plates in a final volume of 200 μl of Baltz medium containing various concentrations of test compounds (tenfold dilutions from 100 μM to 1 pM) and 0.9% DMSO. Wells containing only Baltz medium and 0.9% DMSO served as controls. After 24 h incubation, 20 μl of a 0.5 mM resazurin solution prepared in PBS and sterile filtered was added. Incubation was continued for another 48 h and then the absorbance of the wells was read on a BioTek ELx808 microplate reader using a test wavelength of 570 nm and a reference wavelength of 630 nm. The GI_{50} value (*i.e.* the concentration of a compound necessary to reduce the growth rate of cells by 50% compared to the control) was determined by linear interpolation according to the method described by Huber and Koella [38].

4.4.3. Swelling experiments

Changes in cell volume were measured by the light scattering methods as previously described [20]. Briefly, bloodstream forms of *T. brucei* were incubated at a cell density of $5 \times 10^7 \text{ cells ml}^{-1}$ in 96-well plates in a final volume of 200 μl Baltz medium containing 100 μM ionophore and 0.9% DMSO. Controls contained just 0.9% DMSO. Absorbance of the cultures was measured at 490 nm on a BioTEK ELx808 microplate reader every 10 min for an hour.

Supporting Information

The structures have been deposited with the Cambridge Crystallographic Data Center in the CIF format, no. CCDC 1879997 and 1879998 for **14** and **15**, respectively. Copies of this information can be obtained free of charge from The Director, CCDC, 12 Union Road,

Cambridge, CB2 1EZ, UK (fax: +44 1223 336 033); E-mail: deposit@ccdc.cam.ac.uk or www:
http://www.ccdc.cam.ac.uk.

Additional figures illustrating the mutual overlap of structures **13–15** from scXRD analysis as well as ^1H , ^{13}C and ^{19}F NMR spectra of the newly synthesized compounds are available free of charge *via* Internet at <http://xxx>.

Acknowledgments

M.A. wishes to acknowledge the Polish Science Centre (NCN) for financial support by a SONATA grant (2016/23/D/ST5/00242) and the Foundation for Polish Science (FNP) for a START scholarship.

References

- [1] M. Antoszczak, J. Rutkowski, A. Huczyński, Structure and biological activity of polyether ionophores and their semi-synthetic derivatives, in: G. Brahmachari (Ed.), Bioactive natural products. Chemistry and biology, Weinheim, 2015.
- [2] M. Antoszczak, D. Steverding, A. Huczyński, Anti-parasitic activity of polyether ionophores, Eur. J. Med. Chem. 166 (2019) 32–47.
- [3] H.D. Chapman, Rotation programmes for coccidiosis control, Int. Poult. Prod. 15 (2007) 7–9.
- [4] V. Kaushik, J.S. Yakisich, A. Kumar, N. Azad, A.K.V. Iyer, Ionophores: Potential use as anticancer drugs and chemosensitizers, Cancers 10 (2018) 360.
- [5] M. Antoszczak, A medicinal chemistry perspective on salinomycin as a potent anticancer and anti-CSCs agent, Eur. J. Med. Chem. 164 (2019) 366–377.

- [6] S. Zhou, F. Wang, E.T. Wong, E. Fonkem, T.-C. Hsieh, J.M. Wu, E. Wu, Salinomycin: A novel anti-cancer agent with known anti-coccidial activities, *Curr. Med. Chem.* 20 (2013) 4095–4101.
- [7] C. Naujokat, R. Steinhart, Salinomycin as a drug for targeting human cancer stem cells, *J. Biomed. Biotechnol.* 2012 (2012) 950658.
- [8] P.B. Gupta, T.T. Onder, G. Jiang, K. Tao, C. Kuperwasser, R.A. Weinberg, E.S. Lander, Identification of selective inhibitors of cancer stem cells by high-throughput screening, *Cell* 138 (2009) 645–659.
- [9] S.V. Barrett, M.P. Barrett, Anti-sleeping sickness drugs and cancer chemotherapy, *Parasitol. Today* 16 (2000) 7–9.
- [10] D. Steverding, Sleeping sickness and nagana disease caused by *Trypanosoma brucei*, in: C. Marcondes (Ed.) *Arthropod Borne Diseases*, Springer, Cham, 2017.
- [11] J.R. Franco, P.P. Simarro, A. Diarra, J.G. Jannin, Epidemiology of human African trypanosomiasis, *Clin. Epidemiol.* 6 (2014) 257–275.
- [12] A. Stich, P.M. Abel, S. Krishna, Human African trypanosomiasis, *BMJ* 325 (2002) 203–206.
- [13] G. Cecchi, R.C. Mattioli, J. Slingenbergh, S. De La Rocque, Land cover and tsetse fly distributions in sub-Saharan Africa, *Med. Vet. Entomol.* 22 (2008) 364–373.
- [14] D. Malvy, F. Chappuis, Sleeping sickness, *Clin. Microbiol. Infect.* 17 (2011) 986–995.
- [15] D. Steverding, The history of African trypanosomiasis, *Parasit. Vectors* 1 (2008) 3.
- [16] World Health Organization – Trypanosomiasis, human African (sleeping sickness) [on-line access: 2019–02–18]. [https://www.who.int/en/news-room/fact-sheets/detail/trypanosomiasis-human-african-\(sleeping-sickness\)](https://www.who.int/en/news-room/fact-sheets/detail/trypanosomiasis-human-african-(sleeping-sickness))

- [17] A.H. Fairlamb, Chemotherapy of human African trypanosomiasis: Current and future prospects, *Trends Parasitol.* 19 (2003) 488–494.
- [18] E. Matovu, T. Seebeck, J.C. Enyaru, R. Kaminsky, Drug resistance in *Trypanosoma brucei* ssp., the causative agents of sleeping sickness in man and nagana in cattle, *Microbes Infect.* 3 (2001) 763–770.
- [19] V. Delespaux, H.P. de Koning, Drugs and drug resistance in African trypanosomiasis, *Drug Resist. Updat.* 10 (2007) 30–50.
- [20] D. Steverding, M. Antoszczak, A. Huczyński, *In vitro* activity of salinomycin and monensin derivatives against *Trypanosoma brucei*, *Parasit. Vectors* 9 (2016) 409.
- [21] B. Li, J. Wu, W. Zhang, Z. Li, G. Chen, Q. Zhou, S. Wu, Synthesis and biological activity of salinomycin-hydroxamic acid conjugates, *Bioorg. Med. Chem. Lett.* 27 (2017) 1624–1626.
- [22] M. Antoszczak, K. Popiel, J. Stefańska, J. Wietrzyk, E. Maj, J. Janczak, G. Michalska, B. Brzezinski, A. Huczyński, Synthesis, cytotoxicity and antibacterial activity of new esters of polyether antibiotic – salinomycin, *Eur. J. Med. Chem.* 76 (2014) 435–444.
- [23] M. Antoszczak, E. Maj, J. Stefańska, J. Wietrzyk, J. Janczak, B. Brzezinski, A. Huczyński, Synthesis, antiproliferative and antibacterial activity of new amides of salinomycin, *Bioorg. Med. Chem. Lett.* 24 (2014) 1724–1729.
- [24] T.T. Mai, A. Hamaï, A. Hienzsch, T. Cañeque, S. Müller, J. Wicinski, O. Cabaud, C. Leroy, A. David, V. Acevedo, A. Ryo, C. Ginestier, D. Birnbaum, E. Charafe-Jauffret, P. Codogno, M. Mehrpour, R. Rodriguez, Salinomycin kills cancer stem cells by sequestering iron in lysosomes, *Nat. Chem.* 9 (2017) 1025–1033.

- [25] B. Borgström, X. Huang, M. Pošta, C. Hegardt, S. Oredsson, D. Strand, Synthetic modification of salinomycin: Selective *O*-acylation and biological evaluation, *Chem. Commun.* 49 (2013) 9944–9946.
- [26] M. Antoszczak, A. Urbaniak, M. Delgado, E. Maj, B. Borgström, J. Wietrzyk, A. Huczyński, Y. Yuan, T.C. Chambers, D. Strand, Biological activity of doubly modified salinomycin analogs – Evaluation *in vitro* and *ex vivo*, *Eur. J. Med. Chem.* 156 (2018) 510–523.
- [27] A. Huczyński, M. Antoszczak, N. Kleczewska, M. Lewandowska, E. Maj, J. Stefańska, J. Wietrzyk, J. Janczak, L. Celewicz, Synthesis and biological activity of salinomycin conjugates with floxuridine, *Eur. J. Med. Chem.* 93 (2015) 33–41.
- [28] D. Steverding, A. Huczyński, *Trypanosoma brucei*: Trypanocidal and cell swelling activities of lasalocid acid, *Parasitol. Res.* 116 (2017) 3229–3233.
- [29] K. Merschjohann, F. Sporer, D. Steverding, M. Wink, *In vitro* effect of alkaloids on bloodstream forms of *Trypanosoma brucei* and *T. congolense*, *Planta Med.* 67 (2001) 623–627.
- [30] A. Huczyński, J. Janczak, J. Stefańska, M. Antoszczak, B. Brzezinski, Synthesis and antimicrobial activity of amide derivatives of polyether antibiotic – salinomycin, *Bioorg. Med. Chem. Lett.* 22 (2012) 4697–4702.
- [31] N. Usachova, G. Leitis, A. Jirgensons, I. Kalvinsh, Synthesis of hydroxamic acids by activation of carboxylic acids with *N,N'*-carbonyldiimidazole: Exploring the efficiency of the method, *Synth. Commun.* 40 (2010) 927–935.
- [32] CrysAlis CCD and CrysAlis Red 1.171.38.43, Rigaku Oxford Diffraction, 2015.
- [33] G.M. Sheldrick, Crystal structure refinement with *SHELXL*, *Acta Cryst. C* 71 (2015) 3–8.

- [34] K. Brandenburg, K. Putz, Diamond, Ver. 3.0, Crystal and Molecular Structure Visualization, University of Bonn, Germany (2006).
- [35] H. Hirumi, K. Hirumi, J.J. Doyle, G.A.M. Gross, *In vitro* cloning of animal infective bloodstream forms of *Trypanosoma brucei*, *Parasitology* 80 (1980) 371–382.
- [36] S.J. Collins, R.C. Gallo, R.E. Gallagher, Continues growth and differentiation of human myeloid leukaemic cells in suspension cultures, *Nature* 270 (1977) 347–349.
- [37] T. Baltz, D. Baltz, C. Giroud, L. Crockett L. Cultivation in a semi-defined medium of animal infective forms of *Trypanosoma brucei*, *T. equiperdum*, *T. evansi*, *T. rhodesiense* and *T. gambiense*, *EMBO J.* 4 (1985) 1273–1277.
- [38] W. Huber, J.C. Koella, A comparison of three methods of estimating EC_{50} in studies of drug resistance of malaria parasites, *Acta Trop.* 55 (1993) 257–261.